

Role of Ashwagandha Extract in Ameliorating the Histological and Immunohistochemical Changes in Parotid Gland Induced by Hypothyroidism in Adult Male Rat

Shaimaa Mostafa Kashef and Marwa A. A. Ibrahim

Department of Histology and Cell Biology, Faculty of Medicine, Tanta University, Tanta, Egypt

ABSTRACT

Introduction: Hypothyroidism is a serious health problem worldwide, in which the decrease in the level of thyroid hormone results in a variety of subclinical and clinical symptoms. Salivary glands have an important role in oral hygiene and digestion of food. Any changes in their integrity or activity may influence the patient's health. Ashwagandha is medical herb with antioxidant, anti-inflammatory, antifibrotic, antiapoptotic and antiproliferative activities.

Aim of the Work: To evaluate the histological structural changes induced by hypothyroidism on the parotid gland and analyze the possible protective effect of Ashwagandha against these histopathological changes using various histological and immunohistochemical techniques.

Materials and Methods: Forty adult male albino rats were randomly divided into four main groups: group-I acted as a control group, group-II was given 500 mg/kg/day of aqueous extract of Ashwagandha orally for 30 consecutive days, group-III was given carbimazole orally at dose 1.35 mg/kg/day for 30 consecutive days and group-IV was given both carbimazole and aqueous extract of Ashwagandha in the same dose and manner as group II and group III. The parotid gland specimens were processed for different histological and immunohistochemical techniques. Morphometric and statistical studies were also done.

Results: The hypothyroid group's parotid sections revealed irregular acini, acinar cells have cytoplasmic vacuolization acinar cytoplasmic vacuolations, fibrosis, ductal dilatation, vascular congestion, and nuclear changes. There were increased caspase-3, PCNA and alpha-smooth muscle actin (α -SMA) immune-expressions associated with marked increase in the number of mast cells. On the other hand, Ashwagandha co-treatment prevented most of these histological modifications except for small regions.

Conclusion: Hypothyroidism induced several destructive changes in parotid gland. Ashwagandha had a potent ameliorative role against these changes induced by thyroid dysfunction.

Received: 17 October 2021, **Accepted:** 24 December 2021

Key Words: α -SMA, ashwagandha, hypothyroidism, parotid, PCNA.

Corresponding Author: Shaimaa Mostafa Kashef, MD, Department of Histology and Cell Biology, Faculty of Medicine, Tanta University, Tanta, 31527, Egypt, **Tel.:** +20 10 0827 2320, **E-mail:** shaimaa.kashef@med.tanta.edu.eg

ISSN: 1110-0559, Vol. 46, No. 2

INTRODUCTION

Hypothyroidism is the reduction of the thyroid gland function that subsequently affects the functions of the different body organs. It is a serious health problem that affects both the developing and the developed world with 4-5% prevalence worldwide^[1]. Hypothyroidism is the second most prevalent endocrine condition after diabetes. It is caused by an impairment in the pathways that regulate the synthesis of thyroid hormones or even as a consequence throughout the treatment of hyperthyroidism. Recently, reactive oxygen species (ROS) have been implicated in the etiology of hypothyroidism^[2].

The normal function of the salivary glands is essential for maintaining oral homeostasis. Parotid gland is the largest salivary gland which has a main role in synthesis of the saliva^[3]. Thyroid hormones are crucial for modifying saliva content, production, and secretion as they promote the development of new proteins through DNA transcription. Therefore, the structure of the salivary glands is seriously

impacted with subsequent hyposalivation in hypothyroid patients^[4].

Ashwagandha (*Withania somnifera*) (Ash) is a traditional medicinal herb with different famous names as Indian ginseng. It attracts public attention for its various benefits as it is considered as immunomodulating, anti-inflammatory, antihyperglycemic, and hypolipidemic agent^[5]. Ashwagandha has an antiaging effect with potent antioxidant and anti-inflammatory properties owing to its content of a wide range of polyphenols and flavonoids. In addition to its role in improving muscular weakness, stress, sexual disorders, memory and sleep disturbance^[6]. Previous researches documented the ameliorative effect of the Ashwagandha extract in improving thyroid function by modulating thyroid hormones and minimizing oxidative stress^[5].

Many studies have reported physiological and biochemical changes in the parotid gland as a result of hypothyroid state, but only a few have addressed

histological changes. Therefore, this work aimed to study the possible histological changes in parotid gland of adult male albino rat in experimentally induced hypothyroidism and the potential protective role of Ashwagandha roots extract.

MATERIALS AND METHODS

Animals

Forty adult male albino rats (200–250 g each) were housed in clean, well-ventilated cages that were supplied with 12-hours light/dark cycle and easily access to standard food and water. Just two weeks before experiment, rats were habituated to lab conditions. Local Ethics Committee of Faculty of Medicine at Tanta University in Egypt endorsed the experiment (34729/6/21).

Study design

The rats were randomly divided into four main groups:

Group I (Control group) (n=10): rats were divided into two equal subgroups:

- Subgroup (i): 5 rats received no treatment until the end of the experiment.
- Subgroup (ii): 5 rats received 1ml of distilled water the diluting vehicle for dried powdered roots powder of Ashwagandha and carbimazole for 30 consecutive days.

Group II (Ash group) (n=10): rats received 500 mg/kg/day of aqueous extract of Ash orally for 30 consecutive days^[7].

Group III (hypothyroid group) (n=10): rats were subjected to induction of hypothyroidism according to Ibrahim *et al.*^[8].

Group IV (Ash treated hypothyroid group) (n=10): rats were given aqueous extract of Ash during induction of hypothyroidism as groups II and III respectively.

After 24 hours of the last dose of both treatments, all rats were anesthetized with a 50 mg/kg intraperitoneal injection of sodium pentobarbital^[9]. The parotid glands were rapidly excised, rinsed, and prepared for histological and immunohistochemical study.

Preparation of aqueous extract of Ashwagandha

Dried roots of Ash were supplied in powder form and were purchased from Imtenan, Cairo, Egypt. 20 grams of dry leaf powder were suspended in 100 mL of double distilled water to make the aqueous extract of Ash leaf. The suspension was stirred at 45 ± 5 C overnight then filtered. The resulting filtrate was determined 100% pure water extraction^[10].

Induction of hypothyroidism

Carbimazole is an antithyroid agent that is commercially available in a name of Carbimazole 5 mg Chemical Industries Development Co. (CID), Egypt.

Hypothyroidism was induced by administrating 1.35 mg/kg/day carbimazole dissolved in distilled water for 30 consecutive days by an oral gavage^[8]. Thyroid gland samples from group I (control) and group III (hypothyroid group) were obtained and processed for H&E staining for histomorphological evaluation of the occurrence of hypothyroidism.

Histological staining

Specimens of the parotid gland were fixed in 10% neutral-buffered formalin, dehydrated in ascending grades of alcohol, cleared in xylene, and embedded into soft paraffin. 5 μ m thick parotid sections were cut and stained with:

1. Routine hematoxylin and eosin (H&E) stain for the general examination of tissue^[11].
2. Masson's trichrome stain for detection of collagen fibers^[12].
3. Toluidine blue stain for detection of mast cells^[13].

Immunohistochemical Staining

Immunohistochemical staining were applied via streptavidin-biotin-peroxidase technique using 5- μ m-thick parotid gland sections. The sections were deparaffinized, rehydrated, and placed in a solution of 3% hydrogen peroxide at room temperature for 10 min then immersed in antigen retrieval solution. Next, 10% normal goat serum in phosphate buffered saline solution (PBS) was used for incubation of the sections to prevent non-specific protein binding followed by the addition of antibodies of activated caspase-3 (ab2302; Abcam, USA)^[14], proliferating cell nuclear antigen (PCNA) (sc-56, Santa Cruz Biotech, USA)^[15], and α -SMA primary antibody (1:50) (Abcam, USA)^[16]. A moist chamber was used to incubate the sections overnight at 4°C. Afterwards, drops of streptavidin-peroxidase were added for 30 minutes then rinsed in PBS. Freshly prepared Diaminobenzidine (DAB) solution (as a chromogen) was added to the sections for 5-10 minutes followed by washing in PBS for three changes 2 minutes each then counterstained with Mayer hematoxylin. Light microscope (Olympus, Japan) with a built-in camera was used to examine and photograph all slides in Histology department, Tanta faculty of Medicine.

Morphometric study

Image analysis was performed by using the software Image J (National Institute of Health, Bethesda, Maryland, USA). Ten different non-overlapping fields were randomly selected from each slide per group and quantified at a magnification of 400. Ten different non-overlapping randomly selected fields from each slide at a magnification of 400 were quantified for:

1. The mean area percentage of collagen fibers in Masson's trichrome stained sections^[17].
2. Mean number of mast cells in toluidine blue stained sections^[18].

3. Mean color intensity of caspase-3 positive immunoreaction in DAB-stained sections^[19].
4. Mean percentage of PCNA-positive cells^[20] in DAB-stained sections.
5. Mean area percentage of α -SMA positive cells^[21] and mean color intensity of α -SMA positive immunoreaction in DAB-stained sections^[16].

Statistical analysis

The analysis of the data was done using one-way analysis of variance (ANOVA test) followed the by Turkey's test for comparison between the groups. All values were measured in terms of mean \pm standard deviation. Differences were regarded as significant if probability value $p < 0.05$ ^[22].

RESULTS

Histological results

H&E-stained sections

There were no differences between the structure of parotid glands in adult male rats of control subgroups and the Ash-treated group. Normal parotid tissues were observed as densely packed serous acini and ducts with thin fibrous connective tissue septa in between (Figure 1). A single layer of tall pyramidal epithelial cells encircled a central lumen in serous acini. Numerous striated ducts were observed between the acini, which were lined by a single layer of low columnar epithelial cells (Figure 2).

Concerning H&E stained sections, the control group of thyroid gland was made up of variable- sized follicles with simple cuboidal epithelial cells lining. The thyroid follicles had central lumen that was filled with homogeneous acidophilic colloid (Figure 3).

Regarding the hypothyroid group (group III), thyroid follicles were lined with follicular cells with dark nuclei and highly vacuolated cytoplasm. Disrupted thyroid follicles with desquamated epithelial cell in their lumen were observed. Some other follicles had partially shrunken colloid with congested blood vessels seen between the follicles (Figure 4). Massive destructive changes in the histological architecture of the parotid gland were detected in this group as wide areas of fibrosis surrounding the blood vessels (Figure 5), massive mononuclear cellular infiltration, and dilated congested blood vessels (Figures 5,6,7). Irregular acini had cytoplasmic vacuolation (Figures 6,7) with nuclear changes as irregular nuclei and nuclear margination, and interstitial hemorrhage (Figure 6) were observed. Some interlobular ducts were dilated (Figures 5, 6) while others had cytoplasmic vacuolations (Figure 7).

In contrast, Ash treated hypothyroid group (group-IV) showed a similar histological architecture of parotid gland as control group except for few dilated ducts, minimal fibrosis between parotid lobules, few congested blood vessels (Figure 8), and minimal vacuolization of some acini (Figures 8,9).

Masson's trichrome results

Sections of the parotid glands of the adult male rats in control group showed minimal amount of blue-stained collagen fibers in between the lobules of the gland (Figure 10). In contrast, excessive fibrosis between the lobules of the gland and around the blood vessels and ducts was observed in the parotid gland sections of the rats in hypothyroid group (group-III) (Figure 11). Sections of the parotid gland of Ash treated hypothyroid group (group-IV) showed minimal collagen fibers deposited in between its lobules, around blood vessels and ducts (Figure 12).

A significant increase ($p < 0.05$) in the mean area percentage of collagen fiber content of group III was observed in compared to control group via the morphometric analysis. Whereas in group IV, it was significantly reduced ($p < 0.05$) compared with group III (Table 1, Histogram 1).

Toluidine blue stained results

Histological examination of toluidine blue stained sections of adult male albino rats in control group showed few mast cells (Figure 13), while abundant mast cells within the connective tissue between the acini were detected in group III (Figure 14). Number of the mast cells within the connective tissue between the acini were fewer in Ash treated hypothyroid group (group IV) (Figure 15).

Morphometric analysis of the mean number of mast cells in group III depicted a significant increase ($p < 0.05$) compared to control group. Whereas in group IV, they were significantly fewer ($p < 0.05$) than in group III (Table 1, Histogram 1).

Immunohistochemical results

Caspase-3 immunostaining results

Immunohistochemical staining for caspase 3 was applied to observe apoptotic cell populations. A Weak cytoplasmic immunoreaction of anticaspase-3 in all acinar cells and ductal cells was observed in adult male rat parotid gland of group I (Figure 16). A Positive caspase 3 activity was detected as brown granular cytoplasmic immunoeexpression in most of the acinar cells as well as ductal cells in the parotid gland of hypothyroid rats (group III) (Figure 17). On contrast, parotid gland of Ash treated hypothyroid rats (group IV) showed a moderate caspase-3 activity in some acinar cells as well as ductal cells (Figure 18)

Group III exhibited a significant increase ($p < 0.05$) in the mean color intensity of caspase-3 positive immunoreaction as compared to control group via the morphometric analysis. Whereas group IV was significantly downregulated ($p < 0.05$) with respect to group III (Table 1, Histogram 1).

PCNA immunostaining results

The immunohistochemical staining with anti-PCNA was utilized to detect proliferating cells. Control group (group I) showed a weak nuclear immunopositivity expressed in few cells of serous acini while a negative

immunoreactivity was detected in the cells of striated ducts of parotid gland (Figure 19). Abundant positive PCNA positive cells were observed in most serous acini as well as in the striated ducts of the parotid gland of the hypothyroid rats (Figure 20). On the other hand, a strong nuclear immunopositivity expressed in some serous acini while a negative immunoreactivity was detected in the cells of striated ducts was detected in some serous acini and the striated ducts of Ash treated hypothyroid rats (group IV) (Figure 21).

Group III showed a significant increase in the mean percentage of PCNA positive cells ($p<0.05$) compared to control group via the morphometric analysis. Whereas in group IV it was significantly decreased ($p<0.05$) compared to group III (Table 1, Histogram. 1).

α -SMA immunohistochemical staining

Rat parotid glands in control group showed a weak α -SMA positive immunoreaction in the cytoplasm of the myoepithelial cells around the acini and in the wall of the blood vessels, while negative reaction was noticed around the striated duct (Figure 22). Parotid gland sections of hypothyroid rats (group III) exhibited a strong immune expression of α -SMA in the cytoplasm of the myoepithelial cells around the periphery of most serous acini and in the wall of the blood vessels (Figure 23). On contrast, parotid gland of Ash treated hypothyroid rats (group IV) revealed a moderate positive immunoreaction around some serous acini and a strong positive reaction in the wall of the blood vessels (Figure 24).

Group III recorded a significant increase in the mean area percentage and color intensity of α -SMA positive immunoreaction ($p<0.05$) as compared to control group via the morphometric analysis. Whereas both parameters from group IV were significantly dropped ($p<0.05$) than group III (Table 1, Histogram. 1).

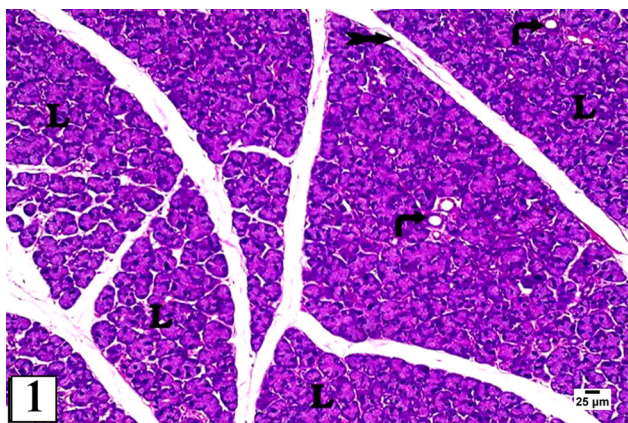


Fig. 1: A photomicrograph of H&E-stained section of an adult male rat parotid gland of the control group (group I) showing its glandular parenchyma in the form of lobules of serous acini (L) and ducts (right angle arrows) with a fine network of interlobular connective tissue (bifid arrow) (H&E×200).

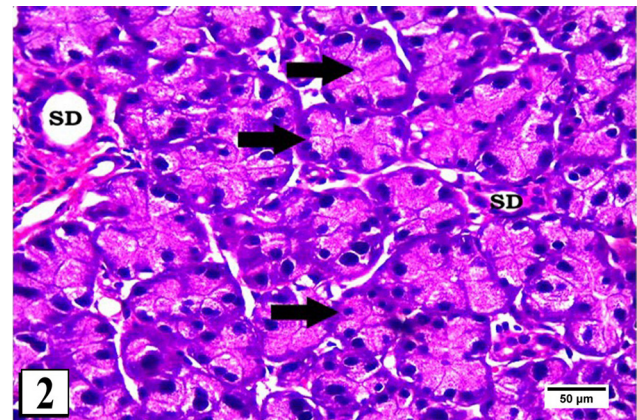


Fig. 2: A photomicrograph of H&E-stained section of an adult male rat parotid gland of the control group (group I) showing pure serous acini having a single layer of pyramidal cells with basal rounded nuclei (thick arrows). Among the acini, striated ducts are observed lined by a single layer of columnar epithelium (SD) (H&E×400).

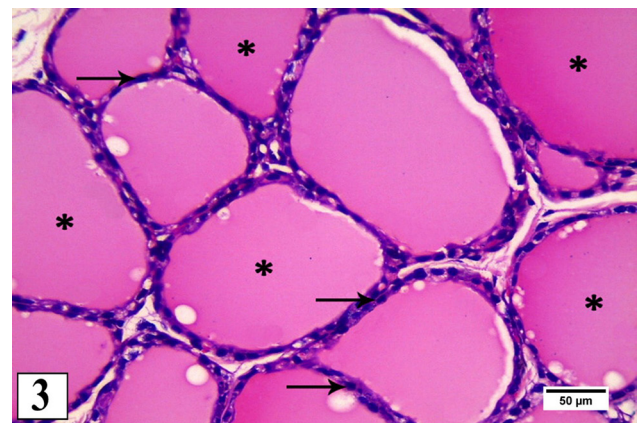


Fig. 3: A photomicrograph of H&E-stained section of an adult male rat thyroid gland of control group (group I) showing variable sized thyroid follicles lined with follicular cuboidal epithelial cells with rounded nuclei (arrows) and filled with homogenous acidophilic colloid (asterisks). (H&E×400).

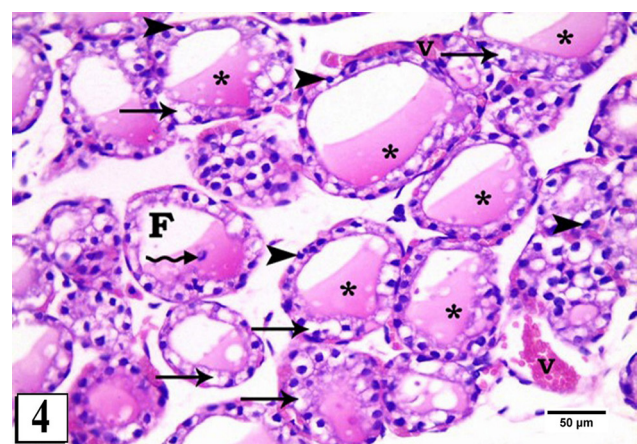


Fig. 4: A photomicrograph of H&E-stained section of an adult male rat thyroid gland of hypothyroid group (group-III) showing thyroid follicles lined with follicular cells with dark nuclei (arrowheads) and vacuolated cytoplasm (thin arrows). Disrupted thyroid follicle (F) with desquamated epithelial cell (wavy arrow) in its lumen is seen. Some follicles have partially shrunk colloid (asterisks). Congested blood vessels (V) are also seen between the follicles (H&E×400).

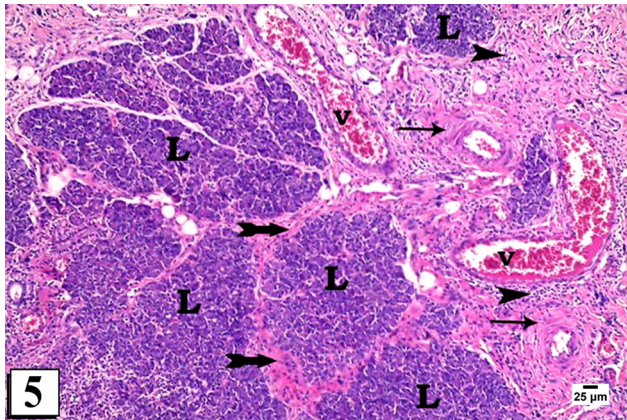


Fig. 5: A photomicrograph of H&E-stained section of an adult male rat parotid gland of hypothyroid group (group-III) showing extensive fibrosis (bifid arrows) in between lobules (L) of parotid gland and perivascular fibrosis (thin arrow). Dilated congested blood vessels (V) and massive cellular infiltration (arrowheads) are noticed (H&E×200).

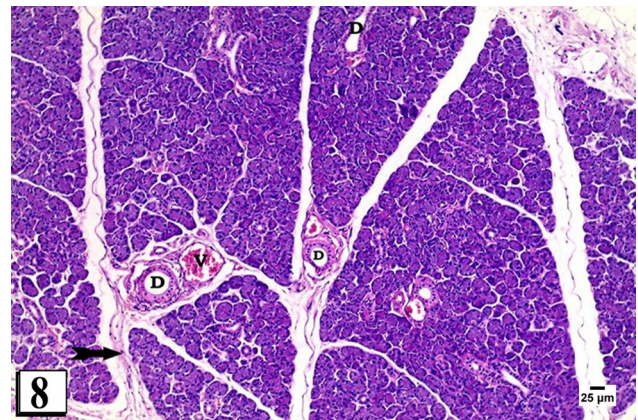


Fig. 8: A photomicrograph of H&E-stained section of an adult male rat parotid gland of Ash treated hypothyroid group (group-IV) showing normal architecture of the parotid lobules except for dilated ducts (D), congested blood vessels (V) and minimal fibrosis between the lobules (bifid arrow) (H&E×200).

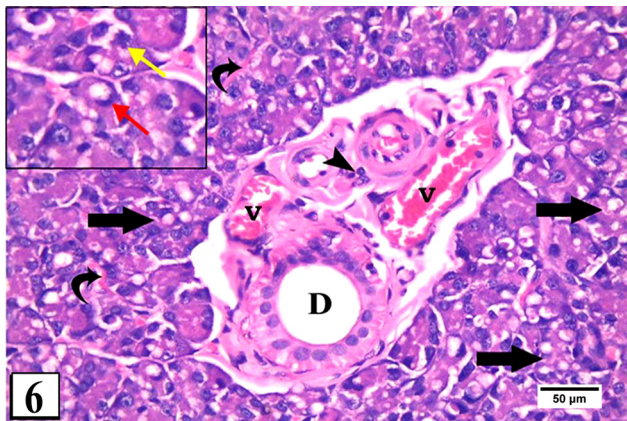


Fig. 6: A photomicrograph of H&E-stained section of an adult male rat parotid gland of hypothyroid group (group-III) showing most of the acini having cytoplasmic vacuolation with irregular outlines (thick arrows). Dilated ducts (D), congested blood vessels (V) are seen with perivascular cellular infiltration (arrow heads) and interstitial hemorrhage (curved arrows). Inset shows margination of the nuclei of serous acini (red arrow) and irregular nuclei (yellow arrow) (H&E×400).

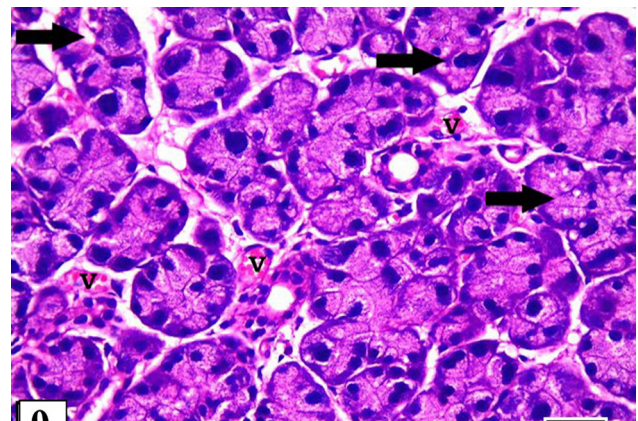


Fig. 9: A photomicrograph of H&E-stained section of an adult male rat parotid gland of Ash treated hypothyroid group (group-IV) showing normal architecture of the parotid acini except for few vacuolated acini (thick arrows) and congested blood vessels (V) (H&E×400).

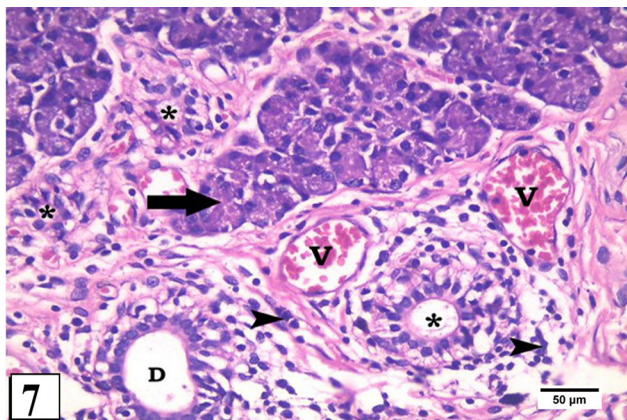


Fig. 7: A photomicrograph of H&E-stained section of an adult male rat parotid gland of hypothyroid group (group-III) showing most of the acini appear irregular (thick arrows). Dilated interlobular duct (D) is seen while other ducts have cytoplasmic vacuolation (asterisks). Congested dilated blood vessels (V) with perivascular cellular infiltration (arrowheads) are noticed (H&E×400).



Fig. 10: A photomicrograph of Masson trichrome stained section of an adult male rat parotid gland of the control group (group I) showing minimal collagen fibers in between its lobules (bifid arrow) (Masson trichrome ×200).

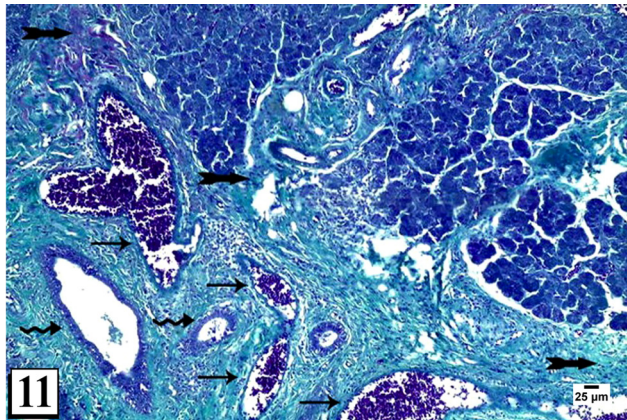


Fig. 11: A photomicrograph of Masson trichrome stained section of an adult male rat parotid gland of hypothyroid group (group-III) showing extensive collagen fibers in between its lobules (bifid arrows), around blood vessels (thin arrows), and ducts (wavy arrows) (Masson trichrome $\times 200$).

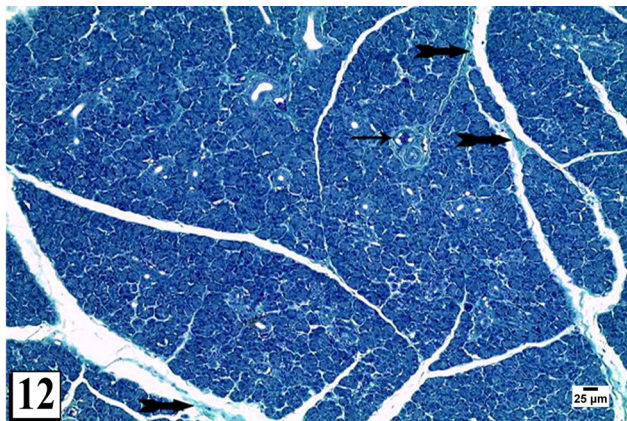


Fig. 12: A photomicrograph of Masson trichrome stained section of an adult male rat parotid gland of Ash treated hypothyroid group (group-IV) showing some collagen fibers in between lobules (bifid arrows) and around blood vessels (thin arrows). (Masson trichrome $\times 200$).

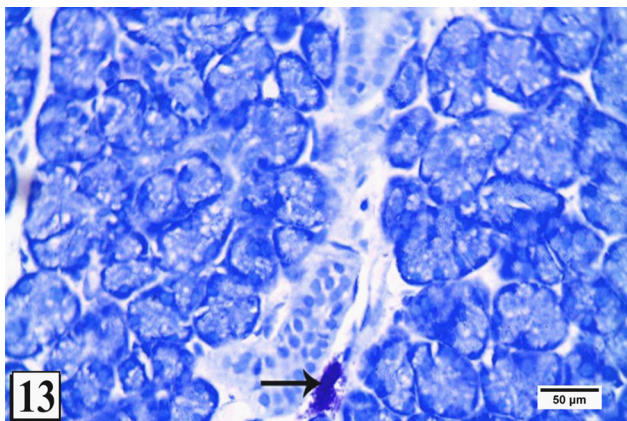


Fig. 13: A photomicrograph of Toluidine blue stained section of an adult male rat parotid gland of the control group (group I) showing few mast cells (thin arrow) within its connective tissue (Toluidine blue $\times 400$).

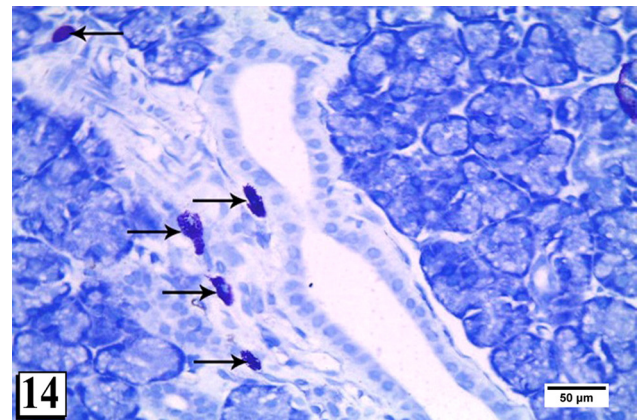


Fig. 14: A photomicrograph of Toluidine blue stained section of an adult male rat parotid gland of the hypothyroid group (group-III) showing abundant mast cells (thin arrows) within its connective tissue (Toluidine blue $\times 400$).

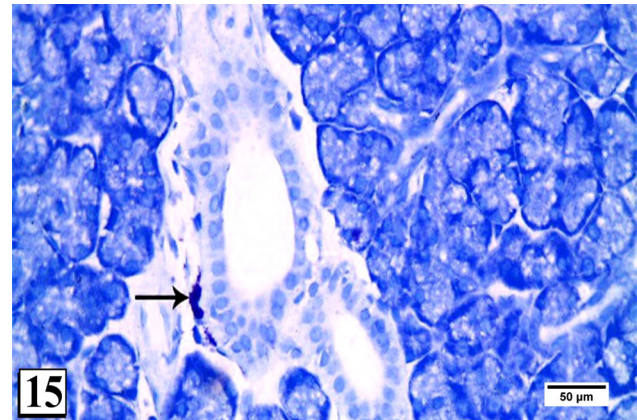


Fig. 15: A photomicrograph of Toluidine blue stained section of an adult male rat parotid gland of Ash treated hypothyroid group (group-IV) showing few mast cells (thin arrow) within its connective tissue. (Toluidine blue $\times 400$).

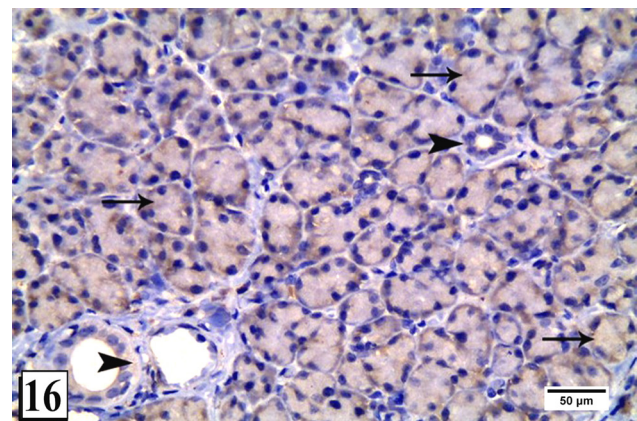


Fig. 16: A photomicrograph of caspase-3 immunostained parotid gland section of an adult male rat control group (group I) showing a weak cytoplasmic caspase-3 immunoreactivity in all serous acini (thin arrows) and ductal cells of the parotid gland (arrowheads) (caspase-3 immunostaining $\times 400$).

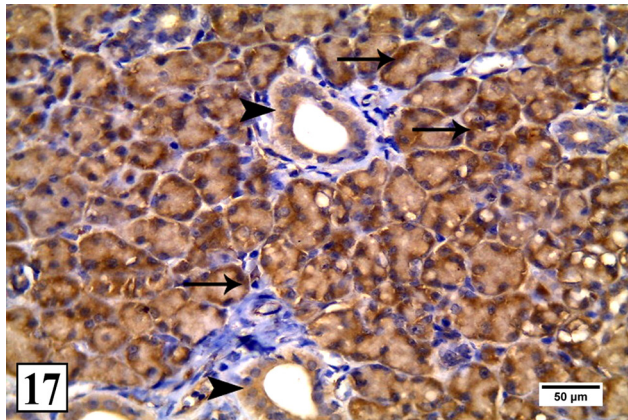


Fig. 17: A photomicrograph of caspases-3 immunostained parotid gland section of the rat hypothyroid group (group-III) showing strong cytoplasmic immunoreactivity for caspases-3 scattered in all serous acini (thin arrows) and ductal cells (arrowheads) (caspase-3 immunostaining x400).

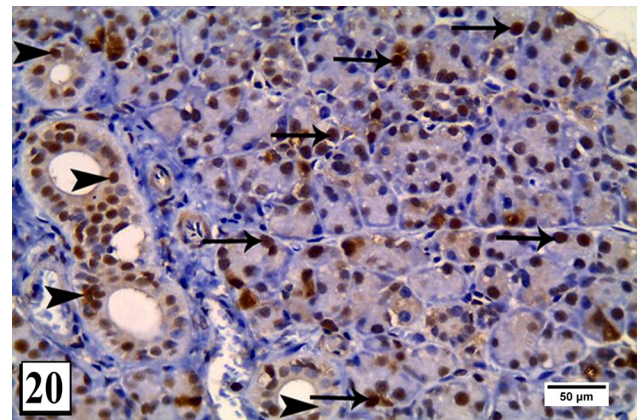


Fig. 20: A photomicrograph of PCNA immunostained parotid gland section of the hypothyroid rat (group III) showing a strong nuclear immunopositivity expressed in most cells of serous acini (thin arrows) and striated ducts (arrowheads) (PCNA immunostaining x400).

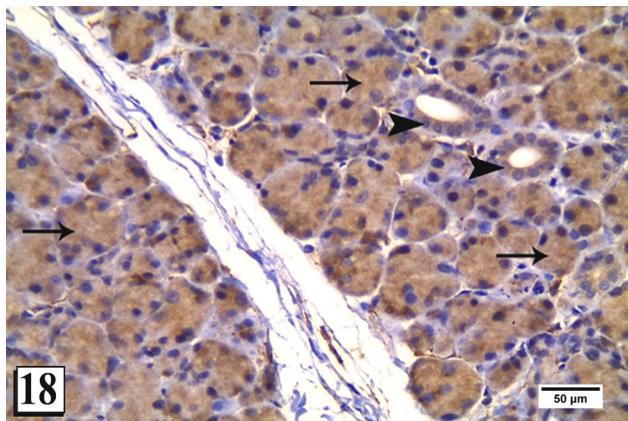


Fig. 18: A photomicrograph of caspases-3 immunostained parotid gland section of Ash treated hypothyroid rat (group-IV) showing a moderate cytoplasmic immunoreactivity for caspases-3 scattered in the cytoplasm of all serous acini (thin arrows) and duct cells (arrowheads) (caspase-3 immunostaining x400).

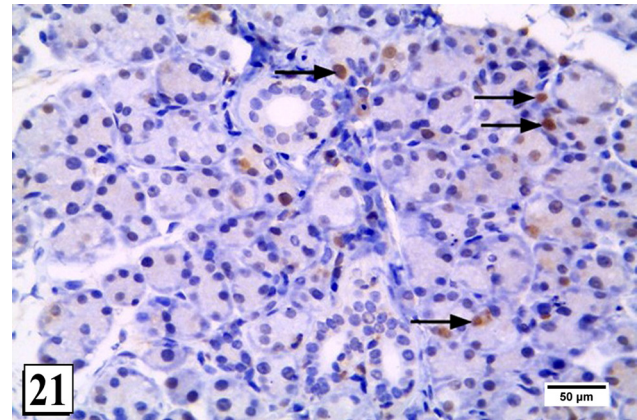


Fig. 21: A photomicrograph of PCNA immunostained parotid gland section of Ash treated hypothyroid rat (group-IV) showing a strong nuclear immunopositivity expressed in some the serous acini (thin arrows) (PCNA immunostaining x400).

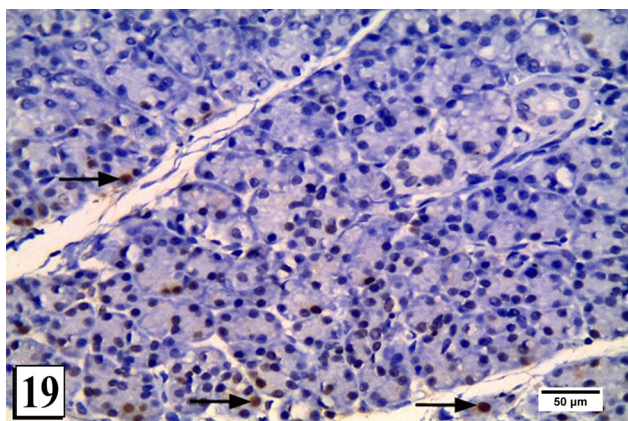


Fig. 19: A photomicrograph of PCNA immunostained parotid gland section of the rat in control group (group I) showing a weak nuclear immunopositivity expressed in few cells of serous acini (arrows) (PCNA immunostaining x400).

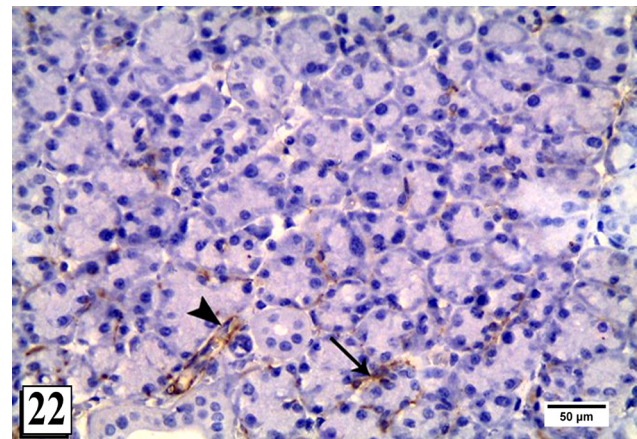


Fig. 22: A photomicrograph of α -SMA immunostained parotid gland section of the adult rat of control group (group-I) showing a weak positive α -SMA immune-expression in the cytoplasm of the myoepithelial cells around the periphery of few serous acini (thin arrows) and in the wall of the blood vessel (arrowheads) (α -SMA immunostaining x400).

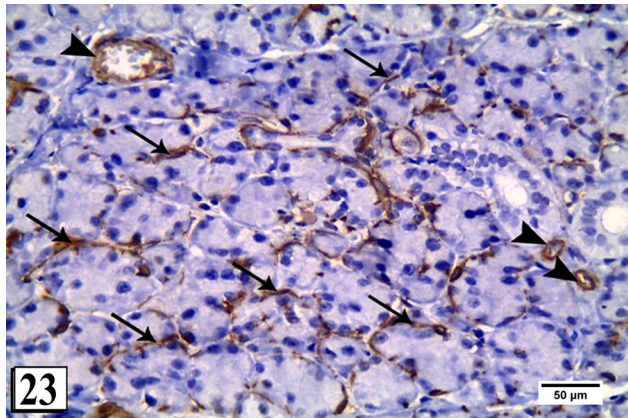


Fig. 23: A photomicrograph of α -SMA immunostained parotid gland section of hypothyroid rat (group-III) showing a strong positive α -SMA immune-expression in the cytoplasm of the myoepithelial cells around the periphery of most serous acini (thin arrows) and in the wall of the blood vessels (arrowheads) (α -SMA immunostaining x400).

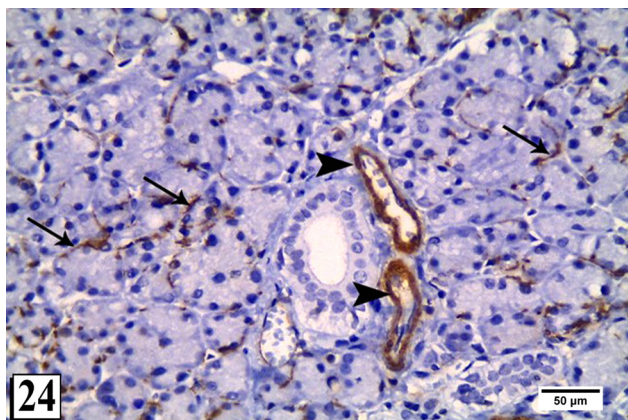
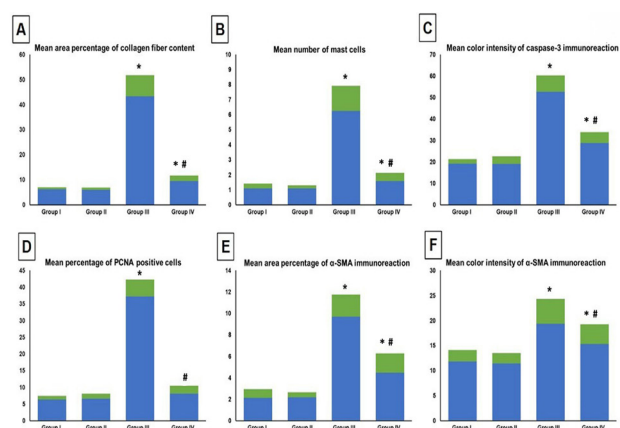


Fig. 24: A photomicrograph of α -SMA immunostained parotid gland section of Ash treated hypothyroid rat (group-IV) showing a moderate positive α -SMA immune-expression in the cytoplasm of the myoepithelial cells around the periphery of some serous acini (thin arrows) and a strong positive immunoreaction appears in the wall of the blood vessel (arrowheads) (α -SMA immunostaining x400).



Histogram 1: Morphometrical and statistical analysis showing: [A] The mean area percentage of collagen fibers content. [B] Mean number of mast cells. [C] Mean color intensity of caspase-3 positive immunoreaction. [D] Mean percentage of PCNA-positive cells. [E] Mean area percentage of α -SMA positive cells. [F] Mean color intensity of α -SMA positive immunoreaction. * indicates significance vs group-I and group-II, # indicates significance vs group III.

Table 1: Morphometric analysis of different study groups

	Group I	Group II	Group III	Group IV
Mean area percentage of collagen fiber content	6.19±0.81	6.07±0.87	43.29±8.42 ^{a,b}	9.54±2.19 ^{a,b,c}
Mean number of mast cells	1.1±0.31	1.09±0.22	6.24±1.68 ^{a,b}	1.59±0.54 ^{a,b,c}
Mean color intensity of caspase-3 positive immunoreaction	19.20±2.11	19.09±3.57	52.66±7.64 ^{a,b}	28.73±5.11 ^{a,b,c}
Mean percentage of PCNA positive cells	6.40±1.09	6.62±1.55	37.21±5.06 ^{a,b}	8.11±2.35 ^c
Mean area percentage of α -SMA positive immunoreaction	2.15±0.80	2.19±0.47	9.68±2.07 ^{a,b}	4.46±1.83 ^{a,b,c}
Mean color intensity of α -SMA positive immunoreaction	11.82±2.30	11.44±2.08	19.37±4.96 ^{a,b}	15.31±3.94 ^{a,b,c}

Data are shown as mean \pm standard deviation. a,b,c indicate significance versus control, Ash-treated, and hypothyroid groups respectively.

DISCUSSION

Hypothyroidism is a serious condition that impacts the structure and function of the salivary glands, particularly the parotid gland. As a result, patients with hyposalivation are primarily evaluated for thyroid dysfunction^[23].

The hypothyroid group of this study revealed histological signs of hypoactivity in the thyroid sections in addition to various histopathological alterations in the parotid gland sections in response to the carbimazole-induced experimental hypothyroidism as nuclear changes, cytoplasmic vacuolation, and signs of inflammation, indicating a successful model of hypothyroidism-induced parotid gland dysfunction. This came as per previous relevant studies^[23,24]. This was attributed to carbimazole-induced drop in the thyroid hormones' levels through iodination blockage of tyrosine residues of thyroglobulin by acting as a false substrate for thyroid peroxidase^[24,25].

Many functional and structural aspects of the parotid gland have been reported to be regulated and controlled by thyroid hormones. Consequently, the high metabolism demands of the parotid gland for proper functioning and secretion of their proteins are not met in hypothyroidism leading to profound parotid alterations, which explains the reversal of most of these changes upon thyroxine replacement^[4,24,26]. Moreover, previous studies reported that inflammation is strongly linked with hypothyroidism due to the raised release of proinflammatory cytokines particularly IL-6^[27]. Nevertheless, various studies strongly proposed oxidative stress development to be responsible

for most of the structural and functional changes occurring upon carbimazole administration^[28,29].

Furthermore, the mean number of mast cells increased significantly in the hypothyroid group of our current study as was similarly reported by other researchers^[30,31]. They attributed this finding to be a part of the inflammatory process and fibrotic changes occurring in the parotid gland, although the exact role of the mast cells could not be clearly elucidated. Nonetheless, researchers strongly linked the increase in mast cell count with the incidence of both benign and malignant tumors of salivary glands^[32].

Additionally, the current study revealed a significant increase in the immunohistochemical expression of α -SMA in the parotid gland of the hypothyroid group to indicate the proliferation of myoepithelial cells, this finding agreed with previous relevant studies^[33,34]. They argued that the proliferation of the myoepithelial cells was a crucial part of the process of the degeneration and regeneration of the acinar cells leading to the surge not only in their number but also in their size as a response to the glandular injury to enhance the cellular compensatory secretion. The significant increase in the collagen fiber deposition may be related to this proliferation of myoepithelial cells. Meanwhile, another study argued that those proliferated myoepithelial cells might not be efficiently functioning as evidenced by the ductal dilatation^[23].

Moreover, the current histological findings were associated with a significant increase in both caspase-3 and PCNA immunohistochemical expression in the parotid gland of the hypothyroid group as was similarly reported by Ayuob^[34], who linked this apoptotic build up to the associated oxidative stress as evidenced by the significant expression of DNA damage, lipid peroxidation, and nitric oxide markers. This also implies that the upregulation of PCNA was a part of the compensatory proliferation to overcome the increased apoptosis.

On the other hand, supplementation of hypothyroid rats with Ashwagandha extract evidently preserved the normal histoarchitecture of the parotid gland, which is most probably linked to its role in restoring levels of thyroid hormones and controlling oxidative stress as reported^[5], where they attributed its potent antioxidant capacity to its high content of polyphenol and flavonoids. Moreover, the synergistic anti-inflammatory role of Ashwagandha extract cannot be ruled out as previously proposed^[35], as this anti-inflammatory action explains the significant reduction in the number of mast cells upon administration Ashwagandha extract, which was linked to the regression of inflammation and fibrosis^[30].

Meanwhile, a significant regression in immunohistochemical expression of α -SMA associating with a significant reduction in collagen fiber content were recorded upon supplementation of hypothyroid rats with Ashwagandha extract. These findings indicated the decrease in the proliferation of myoepithelial cells in response to the preservation of the glandular architecture with subsequent control of fibrosis as previously suggested^[36].

Moreover, in the current work, Ashwagandha extract administration exerted a potent antiapoptotic action as evidenced by a significant decrease in the immunohistochemical expression of caspase-3, which coincided with previous studies^[5,37], who primarily attributed this finding to the potent antioxidant activity of Ashwagandha. Besides, a significant drop in PCNA-positive cells was concurrently reported in the present work. This antiproliferative capacity of Ashwagandha extract has been linked to its content of Withanolides, particularly Withaferin A via its ability to suppress the activation of nuclear factor- κ B^[38,39].

CONCLUSION

Hypothyroidism significantly impacted the histoarchitecture of the parotid gland, which was evidently prevented upon co-administration of Ashwagandha extract. The protective role of Ashwagandha extract is mostly attributed to its antioxidant, anti-inflammatory, antifibrotic, antiapoptotic and antiproliferative activities. More research is needed to determine the most effective dose of Ashwagandha extract for clinical use.

CONFLICT OF INTERESTS

There are no conflicts of interest to declare.

REFERENCES

1. Alam SS. Histological Study of Commiphora mukul, Withania somnifera and Thyroxine in a Murine Model of Hypothyroidism. Proc Shaikh Zayed Med Complex Lahore 2020;34:17–24.
2. Aboul-Fotouh GI, Abou El-Nour RKE-D, Farag E, Boughdady WAE-AA. Histological study on the possible protective effect of curcumin on potassium dichromate induced hypothyroidism in adult male albino rats. Egypt J Histol 2018;41:220–35.
3. Ferreira RO, Aragão WAB, Bittencourt LO, Fernandes LPM, Balbinot KM, Alves-Junior SM, *et al.* Ethanol binge drinking during pregnancy and its effects on salivary glands of offspring rats: oxidative stress, morphometric changes and salivary function impairments. Biomed Pharmacother 2021;133:110979.
4. De Jesus VC, Beanes G, Paraguassú GM, Ramalho LMP, Pinheiro ALB, Ramalho MJP, *et al.* Influence of laser photobiomodulation (GaAIs) on salivary flow rate and histomorphometry of the submandibular glands of hypothyroid rats. Lasers Med Sci 2015;30:1275–80.
5. Abdel-Wahhab KG, Mourad HH, Mannaa FA, Morsy FA, Hassan LK, Taher RF. Role of ashwagandha methanolic extract in the regulation of thyroid profile in hypothyroidism modeled rats. Mol Biol Rep 2019;46:3637–49.

6. Singh SK, Valicherla GR, Bikkasani AK, Cheruvu SH, Hossain Z, Taneja I, et al. Elucidation of plasma protein binding, blood partitioning, permeability, CYP phenotyping and CYP inhibition studies of Withanone using validated UPLC method: An active constituent of neuroprotective herb Ashwagandha. *J Ethnopharmacol* 2021;270:113819.
7. Hosny EN, El-Gizawy MM, Sawie HG, Abdel-Wahhab KG, Khadrawy YA. Neuroprotective Effect of Ashwagandha Extract against the Neurochemical Changes Induced in Rat Model of Hypothyroidism. *J Diet Suppl* 2020;18:72–91.
8. Ibrahim AA, Mohammed NA, Eid KA, Abomughaid MM, Abdelazim AM, Aboregela AM. Hypothyroidism: morphological and metabolic changes in the testis of adult albino rat and the amelioration by alpha lipoic acid. *Folia Morphol (Warsz)* 2021;80:352–62.
9. Ghasi SI, Umana IK, Ogbonna AO, Nwokike MO, Ufelle S. Cardioprotective effects of animal grade piperazine citrate on isoproterenol induced myocardial infarction in wistar rats: Biochemical and histopathological evaluation. *African J Pharm Pharmacol* 2020;14:285–93.
10. Kumar P, Singh R, Nazmi A, Lakhanpal D, Kataria H, Kaur G. Glioprotective effects of Ashwagandha leaf extract against lead induced toxicity. *Biomed Res Int* 2014;2014:182029.
11. Gamble M. The Hematoxylin and Eosin. In: Bancroft, JD and Gamble M, editor. *Theory and Practice of Histological Techniques*. 6th ed. Philadelphia: Churchill Livingstone Elsevier; 2008:121–34.
12. Tumer MK, Cicek M. Differential immunohistochemical expression of type I collagen and matrix metalloproteinase 2 among major salivary glands of young and geriatric mice. *J Appl Oral Sci* 2018; 26: e20170484.
13. Omar A, Yousry M, Farag E. Therapeutic mechanisms of granulocyte-colony stimulating factor in methotrexate-induced parotid lesion in adult rats and possible role of telocytes: A histological study. *Egypt J Histol* 2018;41:93–107.
14. Elwan W. Effect of long-term administration of metanil yellow on the structure of cerebellar cortex of adult male albino rat and the possible protective role of anise oil: A histological and immunohistochemical study. *Egypt J Histol* 2018;41:27–38.
15. Ibrahim MAA, Okasha EF. Effect of genetically modified corn on the jejunal mucosa of adult male albino rat. *Exp Toxicol Pathol* 2016;68:579–88.
16. Abo EL-Yazed AA, EL-sayed SK, EL-Bakary RH, EL-Bakary NA. Histological and Immunohistochemical Study of the Effect of Alendronate on the Submandibular Salivary Gland of Adult Male Albino Rat and the Possible Protective Effect of Propolis. *Med J Cairo Univ* 2018;86:3119–32.
17. Abd El-Haleem MR, Selim AO, Attia GM. Bone marrow-derived mesenchymal stem cells ameliorate parotid injury in ovariectomized rats. *Cytotherapy* 2018;20:204–17.
18. Skopkó BE, Deák Á, Matesz C, Kelentey B, Bácskai T. Pefloxacin induced changes in serotonergic innervation and mast cell number in rat salivary glands. *Drug Chem Toxicol* 2018;43:496–503.
19. Masago R, Aiba-Masago S, Talal N, Zuluaga FJ, Al-Hashimi I, Moody M, et al. Elevated proapoptotic Bax and caspase 3 activation in the NOD.scid model of Sjögren's syndrome. *Arthritis Rheum* 2001;44:693–702.
20. El-naseery NI, Elewa YHA, Ichii O, Kon Y. An experimental study of menopause induced by bilateral ovariectomy and mechanistic effects of mesenchymal stromal cell therapy on the parotid gland of a rat model. *Ann Anat - Anat Anzeiger* 2018;220:9–20.
21. Altayeb Z. Possible Protective Role of Green Tea Extract on Male Rat Parotid Gland in High Fat Diet Induced Obesity (Histological Study). *J Med Histol* 2018;2:69–80.
22. Dawson B, Trapp RG. *Basic & Clinical Biostatistics*. In: *Basic & Clinical Biostatistics*. 4th ed. Lange Medical Books / McGraw-Hill Medical Publishing Division; 2004:162–89.
23. Nasr El-Din WA, Abdel Fattah IO. Histopathological and biochemical alterations of the parotid gland induced by experimental hypothyroidism in adult male rats and the possible therapeutic effect of *Nigella sativa* oil. *Tissue and cell* 2020;65:101366.
24. Abd Elazeem A, Mohammed MZ, Hassan EZ. Effect of Experimentally Induced Hypothyroidism on the Parotid Gland of Adult Male Albino Rats and the possible Role of Thyroid Hormone Supplementation. *Br J Sci* 2016;14:19–36.
25. Cacic-Milosevic M, Korac A, Davidovic V. Methimazole-induced hypothyroidism in rats: Effects on body weight and histological characteristics of thyroid gland. *Jugosl Med Biohemija* 2004;23:143–7.
26. Helal MB, Labah DA, El-Magd MA, Sarhan NH, Nagy NB. Thyroidectomy induces thyroglobulin formation by parotid salivary glands in rats. *Acta Histochem* 2020;122:151568.
27. Mancini A, Di Segni C, Raimondo S, Olivieri G, Silvestrini A, Meucci E, et al. Thyroid Hormones, Oxidative Stress, and Inflammation. *Mediators Inflamm* 2016;2016:6757154.
28. Al-Amoudi W, Mahboub F, Lamfon H, Lamfon N. Assessing induced effect of curcumin on methimazole hepatic damage in albino rats: a histological and histochemical study. *Can J Pure Appl Sci* 2016;10:3961–9.

29. Hassan EG, Adawy HA, Rabea AA. Potential Effect of Carbimazole on Parotid Acini of Albino Rats. *Al-Azhar Dent J Girls* 2020;7:607–10.
30. Hayat N, Nadir S, Rabia DA. Quantitative Comparison of Mast cells in Major Salivary Glands in Hypothyroid State. *J Rawalpindi Med Coll* 2015;201519:263–7.
31. Hashem H, Saad S. Comparative Study of the Effect of Experimentally Induced Hyperthyroidism and Hypothyroidism on the Parotid Gland in Adult Male Albino Rats. *Egypt J Histol* 2020;43:791–807.
32. Jaafari-Ashkavandi Z, Ashraf M-J. Increased mast cell counts in benign and malignant salivary gland tumors. *J Dent Res Dent Clin Dent Prospects* 2014;8:15–20.
33. Mousa AM. Effect of sodium fluoride with and without ginseng on the submandibular gland of adult male albino rat: a histological and immunohistochemical study. *Egypt J Histol* 2011;34:291–301.
34. Ayuob N. Histological and immunohistochemical study on the possible ameliorating effects of thymoquinone on the salivary glands of rats with experimentally induced hypothyroidism. *Egypt J Histol* 2016;39:125–35.
35. Lee W, Kim TH, Ku S-K, Min K-J, Lee H-S, Kwon TK, *et al.* Barrier protective effects of withaferin A in HMGB1-induced inflammatory responses in both cellular and animal models. *Toxicol Appl Pharmacol* 2012;262:91–8.
36. Uzêda-E-Silva VD, Rodriguez TT, Ramalho LMP, Xavier FCA, de Castro ICV, Pinheiro ALB, *et al.* Does laser phototherapy influence the proliferation of myoepithelial cells in the salivary gland of hypothyroid rats? *J Photochem Photobiol B* 2017;173:681–5.
37. Ahmed W, Mofed D, Zekri A-R, El-Sayed N, Rahouma M, Sabet S. Antioxidant activity and apoptotic induction as mechanisms of action of *Withania somnifera* (Ashwagandha) against a hepatocellular carcinoma cell line. *J Int Med Res* 2018;46:1358–69.
38. Li X, Zhu F, Jiang J, Sun C, Wang X, Shen M, *et al.* Synergistic antitumor activity of withaferin A combined with oxaliplatin triggers reactive oxygen species-mediated inactivation of the PI3K/AKT pathway in human pancreatic cancer cells. *Cancer Lett* 2015;357:219–30.
39. Jackson SS, Oberley C, Hooper CP, Grindle K, Wuerzberger-Davis S, Wolff J, *et al.* Withaferin A disrupts ubiquitin-based NEMO reorganization induced by canonical NF- κ B signaling. *Exp Cell Res* 2015;331:58–72.

الملخص العربي

دور مستخلص الأشواجاندا في تحسين التغيرات الهستولوجية والهستوكيميائية المناعية في الغدة النكفية التي يسببها قصور الغدة الدرقية في ذكر الجرذ الأبيض البالغ

شيماء مصطفى كاشف ومروة عوض عبد الحميد ابراهيم

قسم الهستولوجيا وبيولوجيا الخلية - كلية الطب - جامعة طنطا

المقدمة: يعتبر قصور الغدة الدرقية مشكلة صحية خطيرة في جميع أنحاء العالم ، حيث يؤدي انخفاض مستوى هرمون الغدة الدرقية إلى مجموعة متنوعة من الأعراض السريرية. تلعب الغدد اللعابية دورًا مهمًا في نظافة الفم وهضم الطعام وقد تؤثر أي تغييرات في سلامتها أو نشاطها على صحة المريض. الأشواجاندا هي عشب طبي له أنشطة مضادة للأكسدة، وللتهابات، و للتليف، و لموت الخلايا المبرمج، وللتكاثر الخلوي.

الهدف من العمل: تقييم التغيرات الهستولوجية التي يسببها قصور الغدة الدرقية على الغدة النكفية و تحليل التأثير الوقائي المحتمل للأشواجاندا ضد هذه التغيرات باستخدام تقنيات هستولوجية وهستوكيميائية مناعية مختلفة.

المواد والطرق: تم تقسيم أربعين من ذكور الجرذان البيضاء البالغة بشكل عشوائي إلى أربع مجموعات رئيسية: المجموعة الأولى تمثل المجموعة الضابطة ، المجموعة الثانية أعطيت ٥٠٠ مجم / كجم / يوم من المستخلص المائي للأشواجاندا عن طريق الفم لمدة ٣٠ يومًا متتالية ، المجموعة الثالثة أعطيت كاربيمازول عن طريق الفم بجرعة ١,٣٥ مجم / كجم / يوم لمدة ٣٠ يومًا متتالية وتم إعطاء المجموعة الرابعة كلاً من كاربيمازول والمستخلص المائي للأشواجاندا بنفس الجرعات و الطريقة كالمجموعات الثانية والثالثة. تم تجهيز عينات الغدة النكفية للدراسة الهستولوجية و الهستوكيميائية المناعية. كما تم إجراء دراسات قياسية وإحصائية.

النتائج: كشفت مقاطع الغدة النكفية لمجموعة قصور الغدة الدرقية عن وجود عنبيات غير منتظمة ، فجوات في السيتوبلازم ، تليف و تمدد في القنوات، و احتقان الأوعية الدموية ، وتغيرات في الأنوية. كانت هناك زيادة في التعبير الهستوكيميائي المناعي لكل من كاسباس-3 caspase-3 ، و مستضد تكاثر انوية الخلايا PCNA وأكتين العضلات الملساء ألفا (α -SMA) مصحوبة بزيادة ملحوظة في عدد الخلايا البدينة. حافظ العلاج المشترك بالأشواجاندا على معظم هذه التغيرات الهستولوجية باستثناء مناطق صغيرة.

الخلاصة: تسبب قصور الغدة الدرقية في حدوث العديد من التغيرات المدمرة في الغدة النكفية. كان للأشواجاندا دور قوي ضد هذه التغيرات التي يسببها ضعف الغدة الدرقية.